J. Membrane Biol. 127, 21–33 (1992)

The Journal of
Membrane Biology

Quantitative Analysis of Depolarization-Induced ATP Release from Mouse Brain Synaptosomes: External Calcium Dependent and Independent Processes

Jenny L. Fiedler, Harvey B. Pollard, and Eduardo Rojas

Laboratory of Cell Biology and Genetics, National Institute of Diabetes and Digestive and Kidney Diseases, National Institutes of Health, Bethesda, Maryland 20892

Summary. We and others have shown previously that ATP is secreted from mouse brain synaptosomes following depolarization of the membrane by high $[K^+]_o$ and the time course can be monitored accurately by measuring the light emitted from luciferin-luciferase included in the reaction medium. In the present work we have evaluated the relative importance of $[Ca^{2+}]_o$ and membrane potential on the ATP secretion process by modelling the time course of ATP release under different conditions. After correction of the records for destruction of released ATP by synaptosomal ecto-ATPase activity, we found that ATP secretion occurs by an apparent first order process. We also established that, in addition to the classical $[Ca^{2+}]_o$-dependent mode, ATP secretion also occurred in the absence of extracellular calcium ($[Ca^{2+}]_o < 1\ \mu M$). Upon lowering the extracellular Ca^{2+} concentration, both the rate and the extent of ATP secretion decreased. To assess the contribution of membrane potential to the release rate we measured ATP secretion at membrane potentials determined by extracellular $[K^+]_o$ (or $[Rb^+]_o$) as defined by the distribution of the carbocyanine dye, $diSC_3(5)$. Rate constants computed from measured secretion curves revealed that this parameter was essentially independent of membrane potential in the absence of $[Ca^{2+}]_o$. Noise analysis of the light signal showed that the variance increased upon stimulation by high $[K^+]_o$, suggesting that both modes of secretion are quantal. Thus, we conclude that the rate of ATP secretion from nerve terminals depends upon Ca^{2+} entry but not on membrane potential, *per se*.

Key Words ATP secretion · synaptosomes · nerve endings · calcium independent · calcium dependent

Introduction

Exocytosis of ATP from secretory granules in chromaffin cells [6, 22, 24] and pancreatic β-cells [25] can be followed quantitatively in real time by measuring the light emitted from luciferin-luciferase included in the incubation medium. The same method can also be used to measure ATP secretion from synaptosomes from rat brain [31, 32] and squid optic lobe [18] and hippocampal slices [34], although the subcellular origin of ATP secretion in these more heterogeneous systems has not been as well defined. Indeed, the hypothesis that the ATP secreted from synaptosomes might come from synaptic vesicles is based primarily on ATP release data from different cholinergic nerve terminals [11, 14, 26, 29]. In fact, the subcellular basis of transmitter release from the central nervous system remains an unresolved question, the problem being not only the heterogeneity of the secreting terminals, but also the fact that accurate determination of secretion rates depends either on bulk phase samples collected over seconds, or biological assays of postsynaptic changes in electrical potential.

We have therefore examined the secretion of ATP from purified mouse brain synaptosomes [2] in order to assess the role of $[Ca^{2+}]_o$ and membrane potential on both the kinetics and steady-state characteristics of the release process. If ATP secretion were from exocytotic sources rather than cytosolic, then the release might be anticipated to be dependent on $[Ca^{2+}]_o$ and to be quantal. Furthermore, since secretion of transmitter at crayfish or frog neuromuscular junction has been argued to be sensitive to membrane potential, *per se* [1, 17], we have estimated the membrane potential using a fluorescent distribution dye. We find that the rate of ATP secretion is strongly dependent upon $[Ca^{2+}]_o$ but is not affected by membrane potential.

Materials and Methods

Preparation of Synaptosomes

Highly purified synaptosomes from mouse brain were prepared as described elsewhere [2]. In brief, whole brains from a few adult mice were homogenized in cold (ca. 4°C) sucrose buffer (in mM: 320 sucrose, 5 Na-HEPES, pH 7.4) and then centrifuged at

3,000 × *g* for 10 min. The supernatant was centrifuged again at 20,000 × *g* for 20 min to obtain a crude synaptosomal fraction. The pellet was resuspended in sucrose buffer at 4°C, layered on discontinuous metrizamide-sucrose gradient (densities: 1.21, 1.09 and 1.06), and centrifuged at 100,000 × *g* for 75 min. The purified synaptosomal fraction (at the 1.09/1.06 interface) was collected, diluted with sucrose buffer and then centrifuged at 20,000 × *g* for 20 min and finally resuspended in sucrose buffer at a concentration of 1 mg protein per ml.

ATP Detection and Experimental Protocol

ATP secretion from synaptosomes was evoked by a rapid elevation of the $[K^+]_o$ and was monitored continuously by including in the reaction mixture a highly purified preparation of luciferin-luciferase [6, 22, 24]. The contents of a vial (Analytical Luminescence Laboratory, San Diego, CA) of the luciferin-luciferase mixture (referred to as LL) was resuspended in 2 ml of a modified Krebs solution (in mM: 145 NaCl, 5 KCl, 1.2 Mg^{2+}, 1 Ca^{2+}, 10 Na-HEPES, 10 glucose, pH 7.4). The reaction medium for the assay contained 20 μl of the enzyme mixture LL, 5 μl of synaptosomes and a variable volume of Krebs solution (10 to 70 μl) to achieve a constant final volume in the reaction tube of 100 μl after the addition of high $[K^+]_o$ Krebs solution (in mM: 145 KCl, 1.2 Mg^{2+}, 1 Ca^{2+} and 10 K-HEPES, pH 7.4). Before each assay, the synaptosomes were preincubated for 5 min at 30°C in Krebs solution. Sudden increases in $[K^+]_o$, keeping the sum $[Na^+]_o + [K^+]_o$ constant at 155 mM, were achieved by the rapid addition of different volumes of high $[K^+]_o$ Krebs solution. For experiments testing $[Rb^+]_o$ or $[Cs^+]_o$ instead of $[K^+]_o$, high $[Rb^+]_o$ (or high $[Cs^+]_o$) modified Krebs buffer solution was added. The protocol used was similar to that employed with high $[K^+]_o$.

To calibrate the assay, different amounts of ATP dissolved in Kreb's buffer (10 μl) were added after each determination of ATP secretion. ATP secretion in absolute terms, i.e., $pmol_{ATP}/mg_{protein}$, was obtained by measuring total protein present in an aliquot of the synaptosome preparation using bovine serum albumin (BSA) as standard (Bio-Rad assay kit). The total content of ATP present in the aliquot of synaptosomes used in the assay was obtained by the addition of 10 μl of a 10% triton-X-100 solution (ca. 1% final concentration) to the reaction mixture. A final addition of ATP (20 pmol) was used to calibrate the signal.

Data Processing and Analysis

Light emitted by the LL reaction was detected continuously using two photomultipliers with the reaction chamber placed between the photocathodes (*see* Fig. 1*A*). The amplifier circuit used to hold the anode of each photomultiplier to virtual ground was similar to that described elsewhere [6, 22] with a total gain exceeding 10^{16}. The two signals $X(t)$ and $Y(t)$ were filtered (low pass frequency set at 1000 Hz) and recorded using two channels of a video cassette recorder system (PCM/VCR, DX-900 Toshiba, Japan).

Cross correlation analysis of the signals $X(t)$ and $Y(t)$ from two light detectors was carried out using a correlation-probability analyzer (Saicor, model SAI-42A, Honeywell, Denver, CO). For cross-correlation analysis playbacks of the PCM/VCR tapes provided the signals $X(t)$ and $Y(t)$ from the two photomultipliers. The signals $X(t)$ and $Y(t)$ were low pass filtered (200 Hz) and fed to the input amplifiers of the analyzer. The signals $X(t)$ and $Y(t)$ were sampled at 5 msec intervals and were processed by the

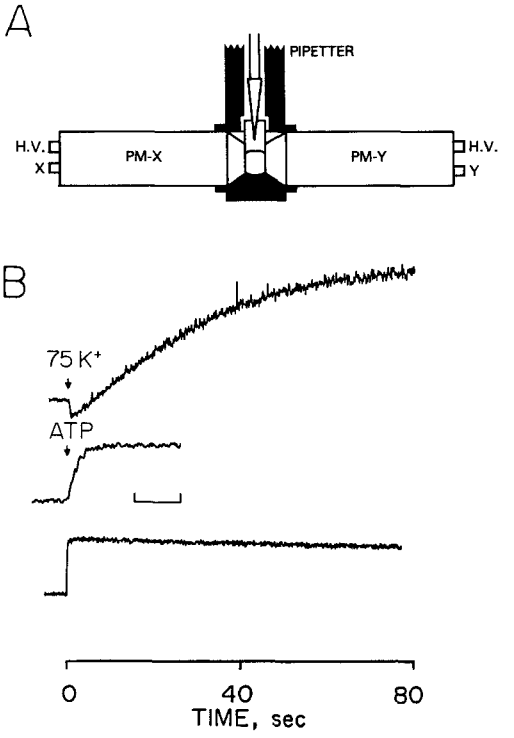

Fig. 1. Determination of mixing time and calibration of the light signal. (*A*) Diagram of the instrument used to measure the light emitted by the LL reaction. The photomultipliers (RCA 8575, RCA, PA) were selected to have similar low noise characteristics. (*B*) Upper record shows the rapid decrease and slow rise in the light signal caused by the injection of 46.7 μl of high $[K^+]$ Krebs solution into 53.3 μl of LL reaction medium containing 5 μl of synaptosomes. Lower record shows the rapid rise in the light signal caused by the injection of 10 μl of KRB solution containing 10 pmol of ATP into 90 μl of LL reaction medium (Krebs solution without synaptosomes). The initial segment of this signal is shown above (time calibration represents 0.3 sec). Temperature throughout, 30°C.

analyzer to calculate a cross correlation function $C_{XY}(T)$ which provides a quantitative measure of the degree of similarity between the two light signals as they are shifted relative to one another in time. The $C_{XY}(T)$ function determined at 100 incremental lag points (5 msec/point) was used to estimate the value at zero shift (representing the variance σ^2 of the signals) and τ_{XY} (representing the average duration of the putative discrete event). The single relaxation time constant model,

$$C_{XY}(T) = \sigma^2 \exp(-T/\tau_{XY}),$$

was used to obtain σ^2 and τ by a least squares regression program.

Records of the secretory response were digitally processed. Each response was digitized into 16,000 points using a digital storage oscilloscope (Nicolet, model 4094B, Nicolet Test Instruments Division, Madison, WI). Each digitized record, representing the base line and the early time course of the ATP secretion in response to high $[K^+]_o$, was transferred to a microcomputer for kinetics analysis. At this stage the points were condensed from 16,000 to 250 points. Since high $[K^+]_o$ inhibits the enzyme

luciferase present in the reaction medium [6], the exact time at which the high $[K^+]_o$ solution was applied could be established by observing the first, nearly instantaneous, decrease in the light emitted by the reaction mixture following the addition of a high $[K^+]_o$ solution. The average of 10 points centered on the minimum value of the 250-point signal (ATP_{min}) was then taken to represent the start (t = 0 sec) of the elevated $[K^+]_o$ (*see* Fig. 1*B*, upper record).

Correction for ATP Degradation Caused by Ecto-ATPase Activity

The luciferin-luciferase technique as used here measures the rate at which light is emitted by the ongoing reaction. It is easy to infer from the rate of reaction how much ATP is present at any given time. Our assay depends on two substrates, namely, luciferin and ATP. Since luciferin is present in excess in the LL mixture, one measures only the time course of the accumulation of the ATP secreted by the synaptosomes. Thus, we expected to observe a monotonic increase in the level of the light signal following the application of high $[K^+]_o$ solution to the synaptosomes. However, most of our records exhibited a rapid increase to a maximum value followed by a relatively slow decay of the light signal. There are several possible explanations for the observed decay, including ATP uptake and ATP hydrolysis by nucleotidases present in the external aspect of the synaptosomal membrane [12, 15, 16].

To correct for the decay, we fitted to each record the following empirical equation

$$ATP(t) = (ATP_{max} - ATP_{min})\,(1 - \exp(-t/\tau))\,\exp(-t/\tau_d) \quad (1)$$

where τ_d represents the time constant of decay and τ represents the time constant of ATP secretion. Accordingly, the reciprocal value of τ_d represents the rate constant of ATP hydrolysis due to ATPase activity other than that of the enzyme mixture LL and any other synaptosomal activity leading to ATP removal from the reaction mixture. Records of the light signal were fitted by the empirical function (Eq. (1)) using a regression program. Three parameters were generated by the program, namely, the difference ($ATP_{max} - ATP_{min}$) representing the extent of the response, the time constant τ representing kinetics of ATP release and τ_d representing the degradation of ATP by ecto-ATPases. To obtain the normalized time course of the ATP release evoked by a sudden elevation in $[K^+]_o$, we first divided each record by ($ATP_{max} - ATP_{min}$) and then added the ATP hydrolyzed by the ecto-ATPases. This was estimated as

$$ATP(t)_{hydrolyzed} = 1 - \exp(-t/\tau_d). \quad (2)$$

Most of the figures illustrating ATP secretion in this paper represent normalized records, i.e.,

$$ATP(t) = (1 - \exp(-t/\tau)). \quad (3)$$

To verify that the decay in the signal was due, at least in part, to the activity of ecto-ATPases known to be present at the external aspect of the synaptosomal membrane [12, 15, 16], we conducted control experiments in which we measured the rate of decay of the light emitted after the addition of ATP (10 pmol) to our reaction medium containing resting intact synaptosomes. The

Table. Effect of external calcium concentration on ecto-ATPase activity present on the surface of intact synaptosomes

$[Ca^{2+}]_o$ (mM)	ATP hydrolysis (pmol/sec)
0.0	0.018 ± 0.002
0.1	0.030 ± 0.003
0.2	0.027 ± 0.003
0.4	0.050 ± 0.004
0.8	0.066 ± 0.007

For each determination a fixed amount of ATP (10 pmol) was rapidly added to the reaction medium containing nonstimulated synaptosomes and LL mixture. The rate of hydrolysis was taken as the rate of decay of the light signal. All reactions were carried out at 30°C. Data presented as mean rate of hydrolysis ± SD (n = 3 per calcium concentration).

Table shows that the rate of decay of the added ATP augmented with $[Ca^{2+}]_o$. This result confirms previous observations in other preparations [12, 15, 16] and suggests that a $[Ca^{2+}]_o$-dependent ATPase activity is present in our highly purified preparation of intact synaptosomes. Although $[Ca^{2+}]_o$-dependent ATP uptake cannot be ruled out, previous efforts to show such a mechanism have produced negative results [33].

Membrane Potential Measurements

To estimate the relationship between membrane potential and $[K^+]_o$ we used the recently introduced [5, 13] carbocyanine dye 3,3′-dipropyl-thiadicarbocyanine iodide ($DiSC_3(5)$; Molecular Probes, Eugene, OR). This dye was excited at 620 nm and the fluorescence was measured at 670 nm. The measurements were carried out using a Spex spectrofluorimeter (Spex Industries, Edison, NJ). For each assay, first we added the dye $DiSC_3(5)$ to 2 ml of Krebs buffer in the cuvette at 30°C (final concentration 0.4 μM). The recording was started with just Krebs buffer (5 mM KCl) to set the zero level of fluorescence. With the addition of the dye the fluorescence rose to ca. 50% of the maximum value. With the addition of an aliquot of the synaptosomal preparation (ca. 100 μg protein), the fluorescence fell to a new level, above the level obtained with the Krebs buffer alone. The observed decrease in fluorescence is due to quenching of the light emitted by the dye. Since quenching of the light emitted by the dye occurs inside the synaptosomes, this result indicates that the presynaptic terminals prepared by us were intact. Prior to the application of high $[K^+]_o$ Krebs buffers, a few measurements were made to form a base line. In some aliquots of synaptosomes, valinomycin, a specific K^+ carrier, was added to obtain the Nernst potential corresponding to the resting K^+ gradient ($[K^+]_o$ = 5 mM). It was noted that the resting $DiSC_3(5)$ fluorescence did not change after the addition of valinomycin in all synaptosomal preparations examined. The $DiSC_3(5)$ fluorescence intensity from resting synaptosomes treated with valinomycin corresponds to F_{min} in Eq. (4). In other aliquots, high $[K^+]$ Krebs buffer was added several times ($[K^+]_o$ adjusted to 25, 45, 65 and 85 mM), and finally, gramicidin, which forms nonselective monovalent cation channels, was applied to give the maximum signal (F_{max}). Normalized steady-state values of fluorescence at different $[K^+]_o$ were calculated as

$$F = \{F - F_{min}\}/\{F_{max} - F_{min}\}. \quad (4)$$

Normalized values of the signal were then plotted against the logarithm of $[K^+]_o$ (*see* Results). Similar protocols were used for the experiments using Rb^+ and Cs^+ as depolarizing agents.

Results

Relationship Between $[K^+]_o$ and Synaptosomal Membrane Potential

One of the aims of this work was to determine any possible effects of membrane potential on the rate of ATP release from presynaptic terminals. To measure the effects of membrane potential on the rate of ATP secretion, it is necessary to establish the relationship between $[K^+]_o$ and membrane potential in our preparation of synaptosomes. To determine such a relationship we have used the distribution dye $DiSC_3(5)$ to monitor and to estimate the changes in potential associated with changes in $[K^+]_o$ [5, 13]. In parallel but separate experiments carried out under similar ionic conditions we have also measured the time course of ATP release. The synaptosomal membrane potential V_m was controlled at four different values in the range from −85 and 0 mV by adjusting $[K^+]_o$ to 25, 45, 65 and 85 mM. The records of changes in fluorescence intensity associated with two successive additions of high $[K^+]_o$ Krebs buffer and gramicidin to the reaction medium containing both synaptosomes and dye are shown in Fig. 2 (upper left side). Following each addition of high $[K^+]$ Krebs buffer, a higher steady-state level of fluorescence was achieved within 25 to 30 sec. The first addition of high $[K^+]$ buffer increased $[K^+]_o$ from 5 to 65 mM and the second addition to 85 mM. In other experiments different $[K^+]_o$ (25 and 45 mM) were tested. Application of gramicidin caused a further increase in fluorescence (F_{max}). Since gramicidin forms nonselective cation channels across the membrane of the synaptosomes, the resting potential can be safely assumed to be close to 0 mV. Under these conditions the concentration of the dye must be equal inside and outside the synaptosomes and maximum fluorescence should be recorded. Conversely, minimum fluorescence is achieved at physiologic $[K^+]_o$ of 5 mM, when the synaptosomal membrane potential is close to the Nernst potential for K^+ ions inside and outside the nerve endings. Under these conditions we expect the concentration of the dye inside the synaptosomes to be greater than that outside causing quenching of the fluorescence. It should be mentioned here that the level of fluorescence was not affected by the addition of valinomycin in the presence of physiologic $[K^+]_o$, i.e., 5 mM (*not shown*). The meaning of this result is that with a physiologic gradient across the synaptosomal membrane, the diffusion potential generated by the activity of the endogenous membrane resident K^+ channels is identical to that generated by the incorporated exogenous K^+ carrier valinomycin molecules. This level of fluorescence was taken as F_{min} and was taken as zero fluorescent intensity (left side vertical axis). The size of the fluorescent signal calculated with Eq. (4) from synaptosomes loaded with the dye (right side vertical axis) was found to be linearly related to the logarithm of $[K^+]_o$ (Fig. 2, ●). Ignoring any possible contribution by

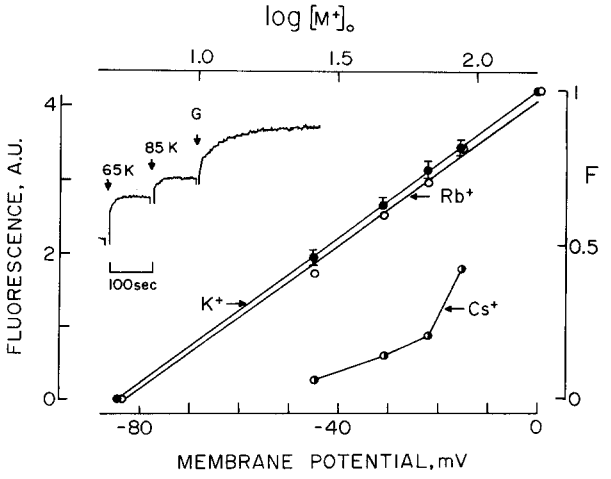

Fig. 2. Membrane potential measurement using the distribution dye Di-S-$C_3(5)$. Vertical axis represents dye fluorescence in arbitrary units. F_{min} and F_{max} were taken as 0 and 4.3 arbitrary units, respectively. *Insert:* Four segments of a continuous record of the $diSC_3(5)$ fluorescence (for calibration use left side vertical axis) from a typical experiment. After a brief base line, two consecutive elevations of $[K^+]_o$ from 5 to 65 and 85 mM were applied. The last segment (*G*) illustrates the change in fluorescence evoked by the addition of gramicidin (final concentration ca. 1 μM). All measurements were carried out at 30°C. Top horizontal axis represents $_{10}\log [M^-]_o$ and M^- stands for either K^+, Rb^- or Cs^-. Data points represent mean values of normalized fluorescence intensity values ± SD ($n = 6$; three different preparations) calculated with Eq. (4) (right side vertical axis). $[K^+]_o$ was increased from 5 mM to 25, 65 and 85 mM, respectively. AT 5 mM $[K^-]_o$ the fluorescence intensity did not change significantly after the addition of valinomycin. The bottom horizontal axis was calculated as

$$V_m = 59.2 \text{ mV } {}_{10}\log \{[K^-]_o/[K^-]_i\}.$$

The fitted straight line intercepted the top axis at 166 mM (representing $[Na^-]_o + [K^-]_o$) and the bottom axis at −85 mV. Symbols as follows: ●, K^-; ○, Rb^- and, ◑ Cs^-. The difference between the slopes of the fitted straight lines through the high $[K^-]_o$ (2.71 a.u. per decade change in concentration in mM) and high $[Rb^-]_o$ (2.62 a.u.) data points was not statistically significant. $[K^-]_i$ was assumed to remain constant at 140 mM.

the anions to the synaptosomal membrane potential (*see* last section of Results), we can calculate V_m at each $[K^+]_o$ using the Nernst equation. Figure 2 also shows the empirical relationship between the normalized values of the fluorescence intensity (F; right vertical axis) and V_m in mV (lower axis). The fitted straight line was calculated by taking into account six values of fluorescence F, four obtained in the presence of high $[K^+]_o$, one obtained in presence of valinomycin ($F = 0$) and one in the presence of gramicidin ($F = 1$). The intercept of 2.22 (upper horizontal axis) corresponds to the logarithm of the estimated value of $[K^+]_o$ plus $[Na^+]_o$ outside (i.e., $10^{2.22} \times 166$ mM). This value is in close agreement with the actual concentration of 155 mM ($= [K^+]_o + [Na^+]_o$) present in the Krebs saline. Taking 166 mM as the sum of the concentration of all intracellular monovalent cations ($[K^+]_i + [Na^+]_i$) and, assuming that $[Na^+]_i$ is ca. 26 mM, the resting membrane potential at 5 mM $[K^+]_o$ is estimated as -85.4 mV ($= 59.2$ mV $_{10}\log \{5/140\}$).

Previous observations using a similar technique suggest that the potential across the membrane of pinched-off presynaptic nerve terminals is a true K^+ diffusion potential [3]. Since membrane resident K^+ channels in many different cell types are also permeant to other monovalent cations, we tested the ability of Rb^+ and Cs^+ to depolarize the membrane of our synaptosomal preparation. Figure 2 also shows the dependence of the membrane potential on external concentration of either Rb^+ (○) or Cs^+ (◑). As expected, Rb^+ is as effective as K^+ in depolarizing the membrane. In contrast, Cs^+, a known blocker of K^+ channels, is substantially less effective in depolarizing the synaptosomes, reaching ca. -50 mV at about 100 mM (◑). Taken together, these results suggest that the membrane potential in isolated presynaptic terminals, purified using metrizamide gradients, is indeed a K^+-diffusion potential across open K^+-selective channels. Thus, our results validate the "chemical voltage-clamp" method for controlling the membrane potential by adjusting $[K^+]_o$ (or $[Rb^+]_o$).

Time Course of K^+-Evoked ATP Secretion from Synaptosomes

Figure 3 (upper panel) illustrates a typical secretory response from purified mouse brain synaptosomes. ATP secretion was evoked by a rapid elevation of $[K^+]_o$ from 5 to 102 mM in presence of 0.5 mM $[Ca^{2+}]_o$. ATP secretion started immediately after the application of high $[K^+]_o$. The signal reached a maximum value 9 sec after the elevation of $[K^+]_o$. Thereafter, a constant decay of the signal was observed ($\tau_d = 43.7$ sec for Fig. 3, upper panel), indicating that one of the substrates of the reaction, namely ATP, was degraded at a constant rate. It should not be forgotten that luciferin in the LL mixture was present in excess and, therefore, its oxidation could not result in measurable changes in the size of the light emitted. Thus, ATP degradation by another ATPase not included in the LL mixture must be the cause for the observed decay of the signal.

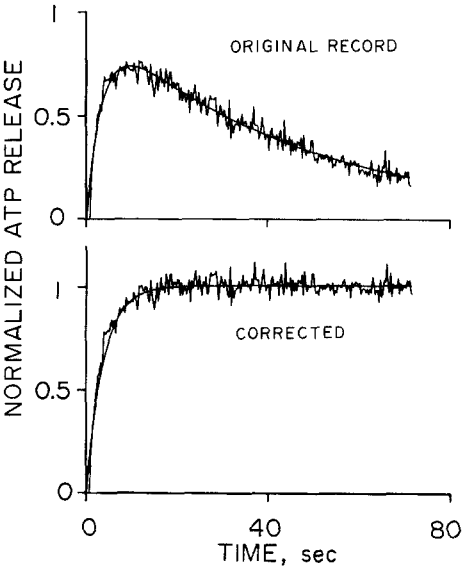

Fig. 3. Time course of ATP release evoked by a rapid elevation of the external potassium. Synaptosomes were preincubated in Krebs solution (32 μl final volume) for 5 min at 30°C prior to the application of 68 μl of the high $[K^+]_o$ Krebs solution. Left side: Upper noisy record illustrates a typical response to an elevation of $[K^+]_o$ from 5 to 103.6 mM in the presence of 0.5 mM $CaCl_2$. The noisy record in the lower panel was obtained from the upper record after correction to take into account the ATP hydrolysis due to ecto-ATPase activity (time constant of decay, 43.7 sec). Smooth curves represent fitted curves calculated with Eqs. (1) and (3) for the upper and lower record, respectively. Time constant, τ, for ATP release: 3.7 sec. Vertical axis represents normalized ATP release from the synaptosomes (*see* Materials and Methods).

Considering that the exponential decay of the light signal is due to the degradation of the ATP secreted by the synaptosomes (Table), we manipulated the original record of the emitted light using the empirical protocol described in Materials and Methods to obtain the corrected record shown in Fig. 3 (lower panel). As expected, the time course of the corrected secretory response could be well fitted by an exponential function with a time constant τ of 3.7 sec (smooth solid line).

The extent of the ATP secretion (in pmol/mg protein) was estimated as follows: A linear calibra-

tion curve (size of the light signal as a function of the amount of ATP added to the reaction medium) was used to estimate the amount of ATP actually released by the synaptosomes (2.6 pmol for the experiment in Fig. 3). From the total protein content of a sample of the synaptosomal preparation and from the total ATP released by the detergent triton X-100 after each secretion assay, we estimated that the average ATP content of our synaptosomal preparations was 4.9 ± 0.7 nmol/mg protein (n = 7 different preparations). A sudden rise in $[K^+]_o$ from 5 to 75 mM evoked the release of 127.4 $pmol_{ATP}/mg_{protein}$.

Effect of $[Ca^{2+}]_o$ on Kinetics of ATP Release

The method used here to analyze the time course of ATP secretion enabled us to measure both the true extent of the cumulative ATP secretion and the time constant, τ, of release. Rate constants of ATP secretion were assumed to be equal to the reciprocal value of the time constant obtained as shown in Fig. 4. To distinguish between the effects of $[Ca^{2+}]_o$ from those of the membrane potential changes, we applied a fixed concentration of K^+ (i.e., 75 mM) to depolarize the synaptosomes from −85 to −18 mV (from Fig. 1) and varied $[Ca^{2+}]_o$. As expected, we found that $[Ca^{2+}]_o$ had a profound effect on the rate of ATP secretion. Figure 4 shows three normalized records of cumulative ATP release evoked by a rapid elevation of $[K^+]_o$ from 5 to 75 mM. Lowering $[Ca^{2+}]_o$ from 1 mM (upper record) to 0.01 μM (lower record) reduced the rate of secretion from 0.19 sec^{-1} (τ = 5.3 sec) to 0.013 sec^{-1} (τ = 74 sec).

ATP secretion rate depended on $[Ca^{2+}]_o$ as illustrated in Fig. 5. Assuming two different modes of ATP secretion in which $[Ca^{2+}]$ is the limiting substrate, we can calculate the dependence of the rate of ATP secretion on $[Ca^{2+}]_o$ as

$$k_{ATP} = k_{max-1}([Ca]_o/(K_{D-1} + [Ca]_o)) + k_{max-2}([Ca]_o/(K_{D-2} + [Ca]_o)), \quad (5)$$

where k_{max-1} and k_{max-2} represent the maximum rates of ATP secretion associated with the high and low affinity modes of ATP secretion, respectively. K_{D-1} and K_{D-2} represent the corresponding apparent dissociation constants. It is clear from Fig. 5 that this minimal model accounts for the experimental relationship between the rate constant k_{ATP} (= $1/\tau$) and $[Ca^{2+}]_o$. The apparent K_D values for the components that generated the best fit to the experimental points are 0.9 μM and 0.57 mM, respectively. The inset to Fig. 5 is a plot of the actual k_{ATP} values as a function of pCa. This experiment was repeated three times with similar results.

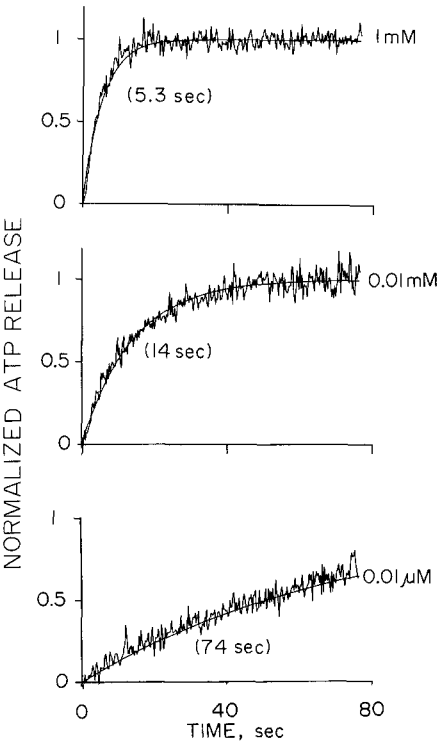

Fig. 4. Effect of the external calcium concentration on kinetics of ATP secretion. Corrected time course of ATP release evoked by high $[K^+]_o$ (75 mM) Krebs solutions (noisy records) with the $[Ca^{2+}]_o$ adjusted using different ratios of $CaCl_2$/NaEGTA: 1 mM (upper), 0.01 mM (middle) and 0.01 μM (lower). Final concentration of EGTA ca. 1 mM. The numbers in parenthesis represent τ values for each condition. Smooth curves represent the best fit of Eq. (3) to the corresponding record. All kinetic measurements were carried out at 30°C. Extent ATP_{max} − ATP_{min} from the fit (% of total ATP in the synaptosomes): 3.3, 2.17 and 1.8 for upper, middle and lower records, respectively.

Effects of $[Ca^{2+}]_o$ on Extent of ATP Release

As illustrated in Fig. 5 (inset), the extent of ATP secretion evoked by a fixed depolarization from −85 to −18 mV (potential values estimated from Fig. 2) augmented from 1.8 to 3.3% of total ATP in the synaptosomes as $[Ca^{2+}]_o$ was increased from 10^{-8} to 10^{-3} M. The relationship between the extent of ATP release and $[Ca^{2+}]_o$ was modelled as for Fig. 5. Thus, the smooth curve in Fig. 6 was calculated as the sum of two modes of ATP release in parallel, i.e.

$$ATP_{total} = ATP_1([Ca]_o/(K_{D-1} + [Ca]_o)] + ATP_2([Ca]_o/(K_{D-2} + [Ca])). \quad (6)$$

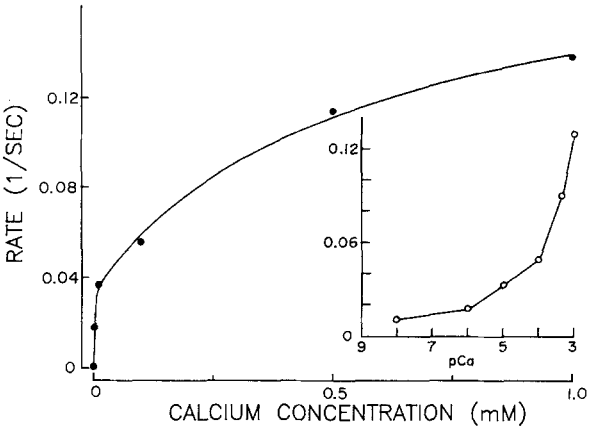

Fig. 5. Relationship between external calcium concentration and rate of ATP release. Vertical axis: Rate of ATP secretion (in sec^{-1}) evoked by 75 mM K^+; Horizontal axis: Concentration of external calcium (in mM). All measurements were carried out at 30°C using aliquots of the same synaptosomal preparation. The experiment was repeated with similar results using two different preparations. The following function was used to fit the experimental points:

$$k = k_{max-1}\{[Ca^{2+}]/(K_{D-1} + [Ca^{2+}])\} + k_{max-2}\{[Ca^{2+}]/(K_{D-2} + [Ca^{2+}])\}$$

where K_{D-1} and K_{D-2} represent dissociation constants for Ca^{2+}-binding sites 1 and 2, respectively. We assumed that the change in ATP secretion rate is proportional to the number of occupied sites. Values for the best fit were as follows: $k_{max-1} = 0.035\ sec^{-1}$; $K_{D-1} = 0.9\ \mu M$; $k_{max-2} = 0.16\ sec^{-1}$; $K_D = 0.57$ mM. pCa values were adjusted using different ratios of $CaCl_2$/NaEGTA. Final concentration of EGTA ca. 1 mM.

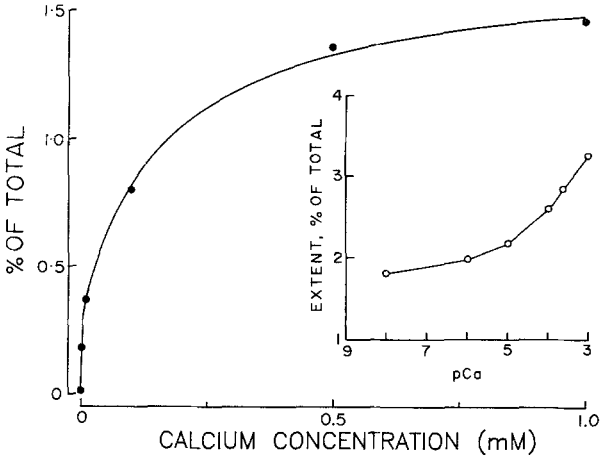

Fig. 6. Relationship between calcium-dependent component of ATP release and external calcium concentration. Left side vertical axis: calcium-dependent component of the ATP release (% of total in the presence of Ca^{2+} minus % of total in the absence of Ca^{2+}) as a function of external calcium concentration in mM. Smooth curve represents the best fit of the following function:

$$ATP = ATP_{max-1}\{[Ca^{2+}]/(K_{D-1} + [Ca^{2+}])\} + ATP_{max-2}\{[Ca^{2+}]/(K_{D-2} + [Ca^{2+}])\}.$$

Parameter values from best fit: $ATP_{max-1} = 0.3\%$; $K_{D-1} = 0.9\ \mu M$; $ATP_{max-2} = 1.36\%$; $K_{D-2} = 0.17\ \mu M$. *Inset:* Extent of ATP secretion (expressed as % of total ATP in the synaptosomes) as a function of pCa.

For this analysis, the extent of ATP release in low calcium (1.8% of the ATP in the synaptosomes) was subtracted from the values obtained at higher calcium concentrations. The maximal extent of the $[Ca^{2+}]_o$-dependent ATP secretion by the high affinity modality ($K_{D-1} = 0.9\ \mu M$) was 0.32% of total ATP in the synaptosomes and that of the low affinity modality ($K_{D-2} = 0.17$ mM) was 1.36% of total ATP in the synaptosomes.

Effects of Membrane Potential on Kinetics and Extent of ATP Release

We have shown that in low calcium ($[Ca^{2+}]_o < 1\ \mu M$), high $[K^+]_o$ can induce ATP release from presynaptic terminals reaching levels as high as 1.8% of the total ATP present in synaptosomes (*see* insert in Fig. 5). Figure 7 depicts typical responses to the application of either high $[K^+]_o$ (left side: 28 mM, upper record; 102 mM, lower record) or high $[Rb^+]_o$ (right side: 28 mM, upper; 102 mM, lower). The time constant of secretion τ changed from 9.9 and 10.1 sec to 8.8 and 9.6 sec for high $[K^+]_o$ and high $[Rb^+]_o$, respectively. Thus, ATP secretion evoked by depolarizing the synaptosomal membrane from −85 to −47 mV (calculated from Fig. 2 for $[K^+]_o = 28$ mM) or to −13 mV (also from Fig. 2 for $[K^+]_o = 102$ mM) occurred at rates of 0.1 and 0.11 sec^{-1}, respectively. Similar results were also obtained when ATP secretion was elicited by high $[Rb^+]_o$. Time constants at different membrane potentials are plotted in Fig. 8 (●: high $[K^+]_o$; □: high $[Rb^+]_o$). It is clear from this figure that the changes in ATP secretion rate are not statistically significant. Thus, we conclude that the kinetics of ATP secretion in the absence of $[Ca^{2+}]_o$ is not affected by membrane potential.

In contrast, the extent of ATP secretion depended on membrane potential as illustrated in Fig. 9. The figure shows the extent of ATP release evoked by high $[K^+]_o$ in the presence of 0.5 mM $[Ca^{2+}]_o$ (●) or $< 1\ \mu M$ $[Ca^{2+}]_o$ (●). To understand the meaning of these data, we applied the Bolzmann's energy model which is often used to determine the voltage dependence of ion channel gating [21]. Accordingly, we fitted a Boltzmann distribution function to both

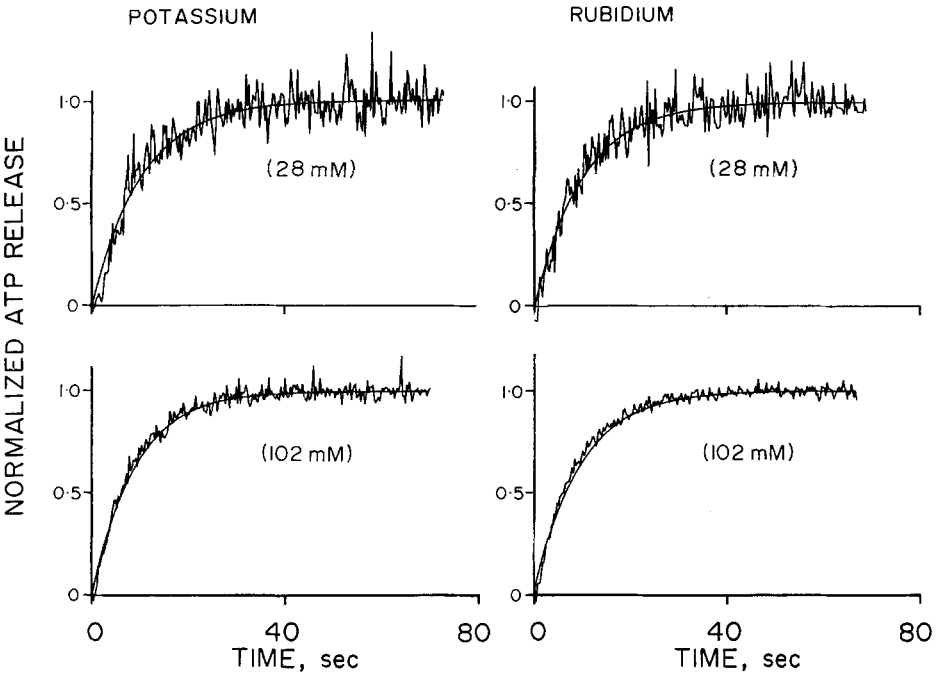

Fig. 7. Effect of membrane potential on kinetics of calcium-independent component of ATP release. Time course of ATP release evoked by a rapid elevation of either $[K^+]_o$ (left side) or $[Rb^+]_o$ (right side) from a typical experiment. Upper panels illustrate the response to an elevation of ion concentration from 5 to 28 mM (extent: 0.28 and 0.39% of total ATP in synaptosomes; τ: 10.1 and 9.95 sec) and, lower panels from 5 to 102 mM (extent: 3.5 and 3.2% of total ATP; τ: 8.8 and 9.6 sec). Mean values (± SD) of extent and time constant for best fit as follows:

	Extent (% of total ATP)	τ (sec)	n
$[K^+]_o$: 28 mM	0.4 ± 0.09	10.13 ± 0.63	3
102 mM	3.5 ± 0.7	8.32 ± 1.26	3
$[Rb^+]_o$: 28 mM	0.34 ± 0.05	10.47 ± 2.96	3
102 mM	3.24 ± 0.9	8.46 ± 0.9	3

sets of points, in the presence and in the absence of $[Ca^{2+}]_o$. The extent of ATP release (vertical axis) is plotted in Fig. 9 as a function of membrane potential (obtained as illustrated in Fig. 2) at each $[K^+]_o$. Smooth curves were calculated as

$$\% \text{ ATP} = \text{ATP}_{\max} [1/(1 + \exp(a[V - V_o]/kT))]$$

where kT equals 24.6 meV at 30°C. a is the effective valence of the sensor and is a measure of the "voltage sensitivity" of the release process. The midpoint potential V_o is a measure of the difference

$$V_o = \psi_i - \psi_o \tag{7}$$

where ψ_i and ψ_o represent inner and outer surface membrane potential, respectively. The parameters a and V_o that gave the best fit were -3.5 electronic charges (ec) and -25 mV in the presence of 0.5 mM $[Ca^{2+}]_o$ and, -2.4 ec and -15 mV in the absence of $[Ca^{2+}]_o$.

As expected from Fig. 2, showing that $[Rb^+]_o$ is as effective as $[K^+]_o$ to control the membrane potential, a rapid elevation of $[Rb^+]_o$ induced ATP secretion both in the presence (*not shown*) and in the absence of external $[Ca^{2+}]_o$ (Fig. 7). We applied Boltzmann's analysis on the data with high $[Rb^+]_o$ in the absence of $[Ca^{2+}]_o$ (Fig. 7, right side). For this set of data, using high $[K^+]_o$ and high $[Rb^+]_o$ to elicit ATP secretion from the same preparation of synaptosomes, the parameter a was ca. -2.4 electronic charges (Fig. 10, upper panel).

As shown in Fig. 10 (lower panel), the extent of secretion evoked by high $[Rb^+]_o$ is linearly related to that evoked by high $[K^+]_o$. The meaning of this result is that both cations are permeant across K^+ channels known to be present in the synaptosomal membrane. The slope of 0.8 of the regression line fitted through the experimental points indicates that,

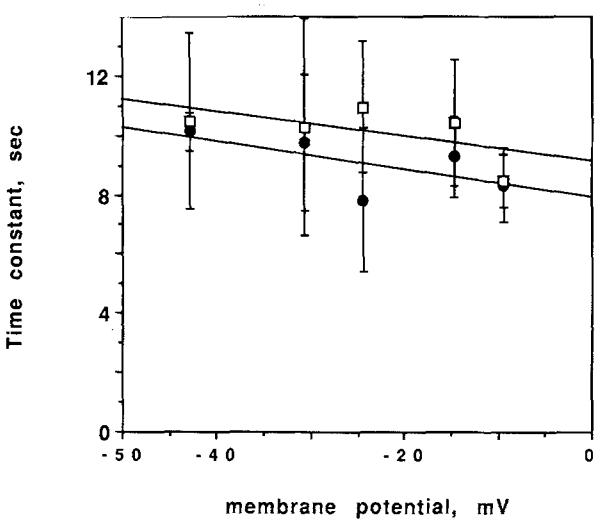

Fig. 8. Relationship between time constant of calcium-independent ATP release and membrane potential. The parameters of the linear regressions are not statistically different. Membrane potentials (horizontal axis) were obtained from Fig. 2. Symbols represent the mean value of 6–9 determinations ± SD from three experiments using different preparations: (●) high $[K^+]_o$ and (□) high $[Rb^+]_o$.

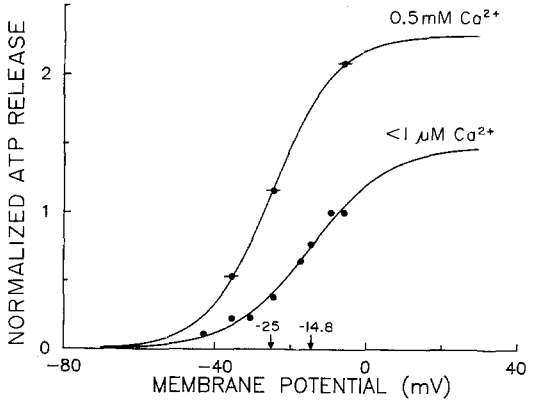

Fig. 9. Analysis of the voltage dependence of the extent of ATP secretion in the presence and absence of calcium. The value representing the extent of the ATP released at −8.9 mV in absence of calcium was used to normalize all the values representing the extent of ATP release in absence (0.1 mM NaEGTA present; ●) and presence of $[Ca^{2+}]_o$ (0.5 mM; -●-). Each symbol represents the mean value from three different synaptosomal preparations. Smooth curves represent the best fit of the Boltzmann's distribution function to each set of points (-●-: 0.5 mM $[Ca^{2+}]_o$; ●: < 1 μM $[Ca^{2+}]_o$). Midpoint potentials (−25 and −14.8 mV, respectively) are shown above the membrane potential axis.

although both cations can be used to depolarize the membrane of pinched-off nerve endings, K^+ is about 20% more effective. It should be mentioned here that, as expected from Fig. 2 showing that Cs^+ is a rather poor depolarizing cation, high $[Cs^+]_o$ was by

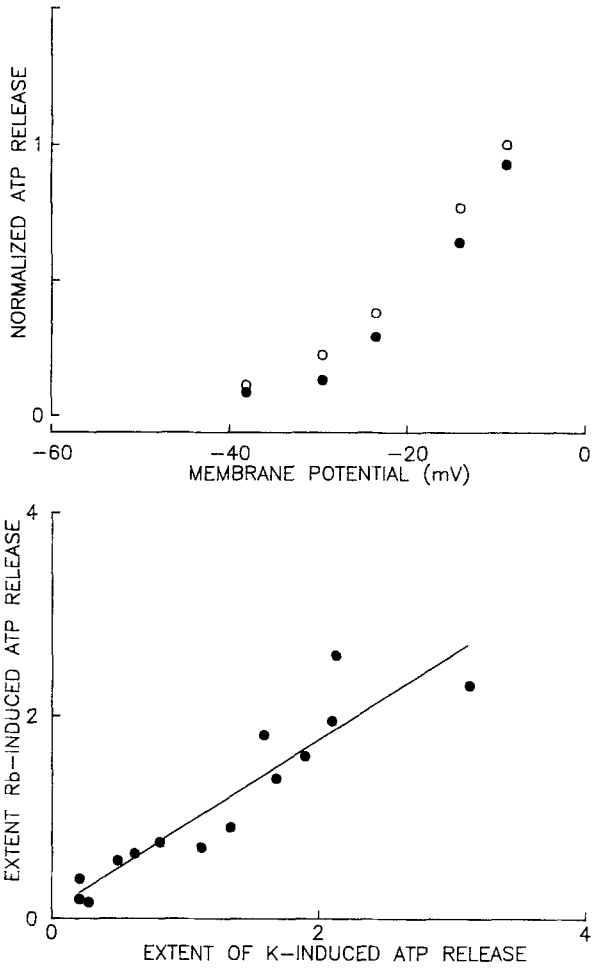

Fig. 10. Voltage dependence of the extent of ATP secretion evoked by high $[K^+]_o$ and high $[Rb^+]_o$ in the absence of calcium. Upper panel: Extent of ATP release as a function of membrane potential adjusted by increasing the external concentration of either K^+ (○) or Rb^+ (●). The value representing the extent of the ATP release evoked by high K^+ at −8.9 mV was used to normalize all values shown in this panel. Lower panel: Extent of ATP release (% of total ATP in the synaptosomes) evoked by high $[Rb^+]_o$ as a function of extent of release evoked by high $[K^+]_o$. Parameters for the fitted straight line: $y = 0.81\,x + 0.12$.

far less effective than high $[K^+]_o$ (or high $[Rb^+]_o$) in causing ATP release. The extent of the release induced by high $[Cs^+]_o$ (98 mM) was ca. one third of that obtained with high $[K^+]_o$ (102 mM; *data not shown*).

ATP Release in the Absence of Calcium is Discrete

We have previously shown that both ACh and high $[K^+]_o$ (*unpublished observations*) evoke ATP secretion from adrenal chromaffin cells and that

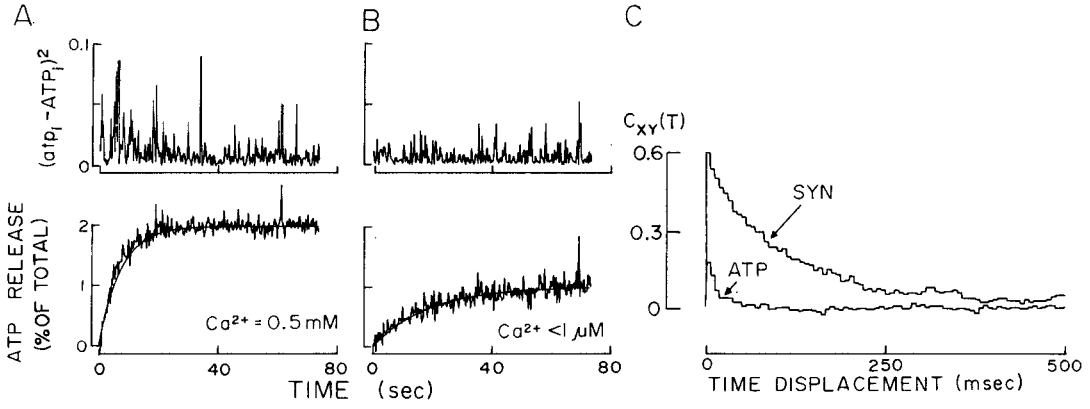

Fig. 11. ATP secretion evoked by membrane depolarization in the absence or presence of added calcium is discrete. (*A,B*) Top panels: Values of δ^2 in the presence of 0.5 mM $[Ca^{2+}]_o$ (left side) or in low $[Ca^{2+}]_o$ (right side). $\sigma^2 (= \Sigma\delta^2)$ values from three different experiments were 1.05, 1.14 and 1.55 (this figure) a.u. in 0.5 mM $[Ca^{2+}]_o$ and 0.77, 1.05 and 0.21 (this figure) a.u. in low $[Ca^{2+}]_o$. Bottom panels: cumulative ATP secretion (% of total ATP in the synaptosomes). (*C*) Vertical axis represents cross correlation values. C_{XY} function labeled *SYN* was calculated from the record in Fig. 1*B* (upper record) after the injection of high $[K^+]_o$ Krebs solution to the LL reaction medium in the presence of synaptosomes. The C_{XY} function labeled *ATP* was calculated from the record of a 10-pmol ATP calibration signal in Fig. 1*B* (lower record). Values of $C_{XY}(T = 0)$ were 0.6 and 0.12 for the functions labeled *SYN* and *ATP*, respectively. The corresponding σ_{XY} values were 150 and 15 msec.

secretion is associated with a marked increase in the variance of the light signal [22]. Noise analysis of the light emitted by luciferin revealed that this excess noise is made up of three main components: photomultiplier noise, intrinsic noise of the luciferin-luciferase reaction, and noise due to the discrete nature of the ATP release process. We concluded that the excess noise due to the discrete nature of the ATP secretion was the predominant component of the variance [22].

To verify the discrete nature of ATP release induced by depolarization of the synaptosomes, we evaluated and compared the values of the variance σ^2 for two segments (80 sec) of the record of the light signal, one prior to the stimulation and the other during the stimulation of the synaptosomes. A computer program calculated the differences between the measured signals (atp_i) and the values (ATP_i) evaluated using Eq. (1). The variance σ^2 was calculated as

$$\sigma^2 = \Sigma\,\delta_i^2 = \Sigma(atp_i - ATP_i)^2. \quad (8)$$

As illustrated in Fig. 11, associated with the secretory activity of the synaptosomes (Fig. 11*A,B*, lower panels), there is a marked increase in the size of δ^2 $(= (atp_i - ATP_i)^2$; Fig. 11*A,B*, upper panels). In the presence of 0.5 mM $[Ca^{2+}]_o$, the mean ($n = 3$) σ^2 $(= \Sigma\,\delta_i^2)$ increased from 0.05 to 1.25 arbitrary units (a.u.). In the absence of external calcium, the mean σ^2 increased from 0.04 to 0.68 a.u. ($n = 3$). Thus, the noise content (as measured by the variance σ^2 of the signal) during the stimulation of the presynaptic endings was significantly higher than under resting conditions.

Figure 11 also illustrates the dependence of the time course of the variance of the signal on $[Ca^{2+}]_o$. It may be seen that the mean value of the individual fluctuations (upper, *A* and *B*) during the initial phase of secretion (<20 sec) is greater in the presence of 0.5 mM Ca^{2+} (Fig. 11*A*) than that in the absence of Ca^{2+} (0.1 mM NaEGTA added; Fig. 11*B*). The variance of the delayed phase of secretion (>60 sec) was similar in the records made in the absence of Ca^{2+} (*B*) and in its presence (*A*).

To further verify that the 10- to 20-fold increase in σ^2 is indeed associated with the discrete nature of the ATP secretion process, we compared the cross correlation function C_{XY} for the signal due to high $[K^+]_o$-evoked ATP secretion (*see* Fig. 1*B*, upper record) with that for the signal caused by the rapid addition of ATP (*see* Fig. 1*B*, lower record). C_{XY} provides a measure of the degree of similarity between the signals from the photomultipliers *X* and *Y* (Fig. 11*C*) as they are shifted relative to one another in time (*T*). The value of C_{XY} at zero shift ($T = 0$) represents the variance σ^2 of the record and τ_{XY} represents the average duration of the putative discrete events. With ATP alone, $C_{XY}(T = 0)$ was equal to 0.18 and τ_{XY} was ca. 15 msec. By contrast, in the presence of synaptosomes, $C_{XY}(T = 0)$ was equal to 0.6 and τ_{XY} was ca. 150 msec. Note that the value of $C_{XY}(T$

= 0) is rather close to the size of the average increase in σ^2 for the records like those shown in Fig. 11*A,B*.

ATP Secretion Evoked by Membrane Depolarization as a Function of the Product $[K^+]_o \cdot [Cl^-]_o$

Membrane depolarization evoked by a rapid elevation of $[KCl]_o$ keeping the osmolarity constant can induce, at least in principle, swelling of the synaptosomes. This swelling may in turn cause ATP release by a process other than exocytosis. Swelling might be induced if K^+ and Cl^- are distributed passively [10]. Then the concentration ratios and the membrane potential under steady-state conditions ought to conform to the relation

$$[K^+]_o/[K^+]_i = [Cl^-]_i/[Cl^-]_o = \exp\{VF/RT\} \quad (9)$$

where $[]_o$ and $[]_i$ indicate concentrations outside and inside the synaptic ending, V is the membrane potential, and F, R, and T have their usual meaning [10]. Equation (9) is applicable only if pinched-off presynaptic nerve endings are permeant to both K^+ and Cl^-. In the absence of information on the relative permeabilities for these two ions, we can assume that this is the case and we can examine the theoretical consequences derived from Eq. (9). Assuming that both K^+ and Cl^- are permeant, under steady-state conditions, the product $[K^+]_o \cdot [Cl^-]_o$ should be equal to $[K^+]_i \cdot [Cl^-]_i$. Thus, immediately after the application of a sudden increase in $[K^+]_o$, the product $[K^+]_o \cdot [Cl^-]_o$ should be substantially greater than $[K^+]_i \cdot [Cl^-]_i$ and, therefore, the initial ionic and osmotic imbalance should drive both Cl^- and water into the synaptosomes, causing swelling. Thus, it is possible that under our low $[Ca^{2+}]_o$ conditions, high external [KCl] might cause ATP molecules to leak out of the pinched-off presynaptic endings. To examine this mechanism, we have repeated a few experiments in low $[Ca^{2+}]_o$ eliciting ATP release by a rise in $[K^+]_o$ from 5 to 40 (or 70) mM. The extent of ATP release at $[K^+]_o$ equal to 40 (or 70 mM) with $[K^+]_o \cdot [Cl^-]_o$ kept constant at 352 ($= 40 \times 8.8 = 70.4 \times 5$) was slightly greater than that obtained with $[K^+]_o \cdot [Cl^-]_o$ at 6,160 ($= 40 \times 154$) or 10,780 ($= 70 \times 154$; *data not shown*).

Discussion

The main contribution of the present work is the introduction of a highly quantitative analytical procedure to study kinetic and steady-state properties of ATP secretion evoked by membrane depolarization from pinched-off presynaptic terminals. Our results show that depolarization of the synaptosomal membrane by rapid elevation of $[K^+]_o$ induces secretion of ATP. In addition to the classical $[Ca^{2+}]_o$-dependent mode, we have found that ATP secretion also occurred in low extracellular calcium (0.1 NaEGTA added; $[Ca^{2+}] < 1$ μM). Although the extent of both modalities of secretion depended on membrane potential, the $[Ca^{2+}]_o$-independent secretion proceeded at a constant rate at all membrane potentials examined. In low $[Ca^{2+}]_o$ the rate of ATP release was substantially smaller than that of the $[Ca^{2+}]_o$ dependent. We propose that the $[Ca^{2+}]_o$-independent ATP release must depend on Ca^{2+} release from intracellular stores [8]. Both the extent and the rate of ATP release were strongly dependent on $[Ca^{2+}]_o$. In addition, we found that increasing $[Ca^{2+}]_o$ from < 1 μM to 0.5 mM increases the steepness of the relationship between extent of ATP release and membrane potential. We interpret this result to indicate that the voltage sensor of the trigger mechanism is located in the membrane and, therefore, can be modulated by changes affecting the inner and outer surface charges.

ATP Secretion Evoked by Membrane Depolarization of Pinched-off Nerve Endings is Discrete

It is well documented that ATP is released from adrenal chromaffin cells together with catecholamines by a $[Ca^{2+}]_o$-dependent exocytotic mechanism [6, 22, 24]. Since acetylcholine (ACh) from mammalian neuromuscular nerve terminals is quantal [7] and, since ATP is cosecreted with ACh in a $[Ca^{2+}]_o$-dependent manner [4], it has been previously assumed that the mechanism of ATP release is also quantal. However, the demonstration of a $[Ca^{2+}]_o$-independent component by us and others [31, 32, 36] makes it mandatory to determine whether the ATP release process in the absence of $[Ca^{2+}]_o$ is also quantal, and thus reflects secretion by exocytosis.

We have shown here that the variance of the light signal, a measure of the noise content is, by and large, caused by the release process of the stimulated pinched-off nerve terminals (Fig. 11*A,B*). Furthermore, the cross correlation analysis of the signals revealed that the excess noise in the records originated from discrete events occurring only if synaptosomes were present in the LL reaction medium. In addition the cross correlation function $C_{XY}(T)$ was found to be exponential, suggesting the presence of events with a single unitary duration. The value at

zero shift, i.e., $C_{XY}(T = 0)$, was equal to 0.6 a.u. in good agreement with the mean value of the variance σ^2 of records obtained at low $[Ca^{2+}]_o$. The time constant τ_{XY} of the cross correlation function, representing the average duration of the putative discrete events, was ca. 150 msec. By contrast, with ATP alone, $C_{XY}(T = 0)$ was equal to 0.18 and τ_{XY} was ca. 15 msec. Taken together, these results strongly support our idea that ATP is released by a discrete process. We may conclude, therefore, that regardless of the presence or absence of Ca^{2+}, ATP secretion must be by exocytosis.

In the case of neurotransmitter release evoked by membrane depolarization in absence of $[Ca^{2+}]_o$ and, to be consistent with the calcium hypothesis for exocytosis, we [8] and others [9] have suggested that the endoplasmic reticulum may be the source of Ca^{2+} for secretion. The idea that secretion in the absence of Ca^{2+} may occur by a mechanism other than exocytosis originated from the inability to resolve a rise in $[Ca^{2+}]_i$ associated with measurable release of endogenous dopamine from striatal synaptosomes [35]. It is possible that the overall increase $[Ca^{2+}]_i$ associated with dopamine release is too small to measure and that secretion observed at reduced levels occurs only in regions near the membrane where the effective concentration of calcium may be sufficient to drive authentic exocytotic release of dopamine [35]. It should be noted that high $[K^+]_o$-induced ATP release in the absence of $[Ca^{2+}]_o$ from both mouse (this work) and rat brain synaptosomes [31] is ca. 50% of that measured in the presence of physiological $[Ca^{2+}]_o$.

Although the origin of the Ca^{2+} required for ATP release induced by membrane depolarization in the absence of external calcium remains to be elucidated, there are a few reports which suggest that activation of phosphoinositide metabolism by membrane depolarization may be involved. The most explicit version of this mechanism can be found in muscle research [23, 30]. In this model membrane depolarization acts directly on phospholipase C which, in turn, acts on phosphatidylinositol 4,5-bisphosphate (PIP_2) with the ensuing generation of inositol 1,2,5-trisphosphate (IP_3) which, in turn, causes Ca^{2+} release from intracellular stores [30].

ATP Secretion as a Marker of Neurotransmitter Release

It is well documented that adenine nucleotides are both costored in presynaptic vesicles and coreleased together with specific neurotransmitters [27, 28]. Indeed, ATP is coreleased in a $[Ca^{2+}]_o$-dependent fashion from electric organ cholinergic nerve terminals [11, 14, 26, 29], from affinity-purified rat brain cholinergic terminals [20] and, from mammalian neuromuscular junction [27]. In addition, several reports show that adenine nucleotides are cosecreted together with specific neurotransmitters from both sympathetic and cholinergic nerve terminals [4]. Consistent with these previous findings, we found that membrane depolarization can elicit ATP secretion from our synaptosomal preparation regardless of the presence or absence of external Ca^{2+}. Our noise analysis has also provided some evidence in support of the idea that the $[Ca^{2+}]_o$-independent modality of ATP release is by exocytosis.

However, the question of whether adenine nucleotides are secreted from specific purinergic nerve terminals in the central nervous system (CNS) remains to be elucidated. Dissociation between ATP and ACh secretion from purified synaptosomes [19, 33], suggest the presence of specific purinergic pathways in the brain. The demonstration of ATP secretion from a highly purified preparation of cholinergic nerve endings from striatum indicates a costorage of ATP with ACh in the basal ganglia [20].

In conclusion, we have established that synaptosomal membrane depolarization evokes ATP secretion and that, in addition to the $[Ca^{2+}]_o$-dependent mode, secretion also occurs in the absence of external calcium. We have also shown that, while the extent of secretion depends on the concentration of external calcium and membrane potential, the rate of secretion depends upon Ca^{2+} entry but not on membrane potential, per se. In addition, our preliminary noise analysis of the light signals suggests that ATP secretion may be discrete regardless of the presence or absence of extracellular Ca^{2+}.

References

1. Arechiga, H., Cannone, A., Parnas, H., Parnas, I. 1990. Blockage of synaptic release by brief hyperpolarizing pulses in the neuromuscular junction of the crayfish. *J. Physiol.* **430:**119–133
2. Bitran, J.A., Rojas, E., Ornberg, R.L., Pollard, H.B. 1992. Quantitative secretion of ATP from mouse brain synaptosomes purified on metrizamide gradients. *Cell. Tissue Res. (Submitted)*
3. Blaustein, M.P., Goldring, J.M. 1975. Membrane potentials in pinched-off presynaptic nerve terminals monitored with a fluorescent probe: Evidence that synaptosomes have potassium diffusion potentials. *J. Physiol.* **247:**589–615
4. Burnstock, G. 1986. Purines as cotransmitters in adrenergic and cholinergic neurones. *Prog. Brain Res.* **68:**193–203
5. Cabrini, G., Verkman, A.S. 1986. Potential-sensitive response mechanism of DiS-C_3-(5) in biological membranes. *J. Membrane Biol.* **92:**171–182
6. Ceña, V., Rojas, E. 1990. Kinetic characteristics of calcium-dependent, cholinergic receptor controlled ATP secretion

from adrenal medullary chromaffin cells. *Biophys. Biochim. Acta* **1023:**213–222
7. Del Castillo, J., Katz, B. 1991. Quantal components of the end-plate potential. *J. Physiol.* **124:**560–573
8. Etcheberrigaray, R., Fiedler, J.L., Pollard, H.B., Rojas, E. 1991. Endoplasmic reticulum as a source of Ca^{2+} in neurotransmitter secretion. *Ann. N.Y. Acad. Sci.* **603:**90–99
9. Gandhi, C.R., Ross, D.H. 1987. Inositol 1,4,5-triphosphate induced mobilization of Ca^{2+} from rat brain synaptosomes. *Neurochem. Res.* **12:**67–72
10. Hodgkin, A.L., Horowicz, P. 1959. The influence of potassium and chloride ions on the membrane potential of single muscle fibers. *J. Physiol.* **148:**127–160
11. Israel, M., Meunier, F.M. 1978. The release of ATP triggered by transmitter action and its possible physiological significance: Retrograde transmission. *J. Physiol.* **74:**485–490
12. Keller, F., Zimmermann, H. 1983. Ecto-adenosine triphosphatase activity at the cholinergic nerve endings of the *Torpedo* electric organ. *Life Sci.* **33:**2635–2641
13. Meunier, F.M. 1984. Relationship between presynaptic membrane potential and acetylcholine release in synaptosomes from *Torpedo* electric organ. *J. Physiol.* **354:**121–137
14. Morel, N., Meunier, F.M. 1981. Simultaneous release of acetylcholine and ATP from stimulated cholinergic synaptosomes. *J. Neurochem.* **36:**1766–1773
15. Nagy, A., Shuster, T.A., Rosenberg, M.D. 1983. Adenosine triphosphatase activity at the external surface of chicken brain synaptosomes. *J. Neurochem.* **40:**226–234
16. Nagy, A., Shuster, T.A., Delgado-Escueta, A.V. 1986. Ecto-ATPase of mammalian synaptosomes: Identification and enzymic characterization. *J. Neurochem.* **47:**976–986
17. Parnas, I., Parnas, H. 1988. The Ca-voltage hypothesis for neurotransmitter release. *Biophys. Chem.* **29:**85–93
18. Pollard, H.B., Pappas, G.D. 1979. Veratridine-activated release of adenosine-5′-triphosphate from synaptosomes: Evidence for calcium dependence and blockade by tetrodotoxin. *Biochim. Biophys. Res. Commun.* **88:**1315–1321
19. Rabasseda, X., Solsona, C., Marsal, J., Egea, G., Bizzini, B. 1987. ATP release from pure cholinergic synaptosomes is not blocked by tetanus toxin. *FEBS Lett.* **213:**337–340
20. Richardson, P.J., Brown, S.J. 1987. ATP release from affinity-purified rat cholinergic nerve terminals. *J. Neurochem.* **48(2):**622–630
21. Rojas, E. 1976. Gating mechanism for the activation of the sodium conductance in nerve terminals. Cold Spring Harbor Symp. Quant. Biol. **40:**305–320
22. Rojas, E., Forsberg, E., Pollard, H.B. 1985. Optical detection of calcium dependent ATP release from stimulated medullary chromaffin cells. *Adv. Exptl. Med. Biol.* **211:**7–28
23. Rojas, E., Nassar-Gentina, V., Luxoro, M., Pollard, M.E., Carrasco, M.A. 1987. Inositol 1,4,5-triphosphate-induced Ca^{2+} release from sarcoplasmic reticulum and contraction in crustacean muscle. *Can. J. Physiol. Pharmacol.* **65:**672–680
24. Rojas, E., Pollard, H.B., Heldman, E. 1985. Real-time measurements of acetylcholine-induced release of ATP from bovine medullary chromaffin cells. *FEBS Lett.* **185:**323
25. Rojas, E., Santos, R., Stutzin, A., Pollard, H.B. 1986. Optical detection of ATP release from stimulated endocrine cells: A universal marker of exocytotic secretion of hormones. *In:* Ionic Channels in Cells and Models Systems. R. Latorre, editor. pp. 163–177. Plenum, New York—London
26. Schweitzer, E. 1987. Coordinated release of ATP and Ach from cholinergic synaptosomes and its inhibition by calmodulin antagonists. *J. Neurosci.* **7:**2948–2956
27. Silinsky, E.M. 1975. On the association between transmitter secretion and the release of adenine nucleotides from mammalian motor nerve terminals. *J. Physiol.* **247:**145–162
28. Su, C. 1983. Purinergic neurotransmission and neuromodulation. *Annu. Rev. Pharmacol. Toxicol.* **23:**397–411
29. Unsworth, C.D., Johnson, R.G. 1990. Acetylcholine and ATP are coreleased from the electromotor nerve terminals of *Narcine brasiliensis* by an exocytotic mechanism. *Proc. Natl. Acad. Sci. USA* **87:**553–557
30. Vergara, J., Tsien, R., Delay, M. 1985. Inositol 1,4,5-triphosphate: A possible chemical link in excitation-contraction coupling in muscle. *Proc. Natl. Acad. Sci. USA* **82:**6352–6356
31. White, T.D. 1977. Direct detection of depolarisation-induced release of ATP from synaptosomal preparation. *Nature* **267:**67–68
32. White, T.D. 1978. Release of ATP from a synaptosomal preparation by elevated extracellular K^+ and by veratridine. *J. Neurochem.* **30:**329–336
33. White, T.D., Potter, P., Wonnacott, S. 1980. Depolarization-induced release of ATP from cortical synaptosomes is not associated with acetylcholine release. *J. Neurochem.* **34:**1109–1112
34. Wieraszko, A., Goldsmith, G., Seyfried, T.N. 1989. Stimulation-dependent release of adenosine triphosphate from hippocampal slices. *Brain Res.* **485:**244–250
35. Woodward, J.J., Chandler, L.J., Leslie, S.W. 1988. Calcium-dependent and -independent release of endogenous dopamine from rat striatal synaptosomes. *Brain Res.* **473:**91–98
36. Zhang, J., Kornecki, E., Jackman, J., Ehrlich, Y.H. 1988. ATP secretion and extracellular protein phosphorylation by CNS neurons in primary culture. *Brain Res. Bull.* **21:**459–464

Received 18 June 1991; 14 November 14 1991